

Organo-Soluble Porphyrin Mixed Monolayer-Protected Gold Nanorods with Intercalated Fullerenes

Chenming Xue, Yongqian Xu, Yi Pang, Dingshan Yu, Liming Dai, Min Gao, Augustine Urbas, and Quan Li

Langmuir, Just Accepted Manuscript • DOI: 10.1021/la300096n • Publication Date (Web): 16 Mar 2012

Downloaded from <http://pubs.acs.org> on March 20, 2012

Just Accepted

“Just Accepted” manuscripts have been peer-reviewed and accepted for publication. They are posted online prior to technical editing, formatting for publication and author proofing. The American Chemical Society provides “Just Accepted” as a free service to the research community to expedite the dissemination of scientific material as soon as possible after acceptance. “Just Accepted” manuscripts appear in full in PDF format accompanied by an HTML abstract. “Just Accepted” manuscripts have been fully peer reviewed, but should not be considered the official version of record. They are accessible to all readers and citable by the Digital Object Identifier (DOI®). “Just Accepted” is an optional service offered to authors. Therefore, the “Just Accepted” Web site may not include all articles that will be published in the journal. After a manuscript is technically edited and formatted, it will be removed from the “Just Accepted” Web site and published as an ASAP article. Note that technical editing may introduce minor changes to the manuscript text and/or graphics which could affect content, and all legal disclaimers and ethical guidelines that apply to the journal pertain. ACS cannot be held responsible for errors or consequences arising from the use of information contained in these “Just Accepted” manuscripts.

Report Documentation Page

*Form Approved
OMB No. 0704-0188*

Public reporting burden for the collection of information is estimated to average 1 hour per response, including the time for reviewing instructions, searching existing data sources, gathering and maintaining the data needed, and completing and reviewing the collection of information. Send comments regarding this burden estimate or any other aspect of this collection of information, including suggestions for reducing this burden, to Washington Headquarters Services, Directorate for Information Operations and Reports, 1215 Jefferson Davis Highway, Suite 1204, Arlington VA 22202-4302. Respondents should be aware that notwithstanding any other provision of law, no person shall be subject to a penalty for failing to comply with a collection of information if it does not display a currently valid OMB control number.

1. REPORT DATE 20 MAR 2012	2. REPORT TYPE	3. DATES COVERED 00-00-2012 to 00-00-2012			
4. TITLE AND SUBTITLE Organo-Soluble Porphyrin Mixed Monolayer-Protected Gold Nanorods with Intercalated Fullerenes		5a. CONTRACT NUMBER			
		5b. GRANT NUMBER			
		5c. PROGRAM ELEMENT NUMBER			
6. AUTHOR(S)		5d. PROJECT NUMBER			
		5e. TASK NUMBER			
		5f. WORK UNIT NUMBER			
7. PERFORMING ORGANIZATION NAME(S) AND ADDRESS(ES) Case Western Reserve University, Department of Chemical Engineering, 10900 Euclid Avenue, Cleveland, OH, 44106		8. PERFORMING ORGANIZATION REPORT NUMBER			
9. SPONSORING/MONITORING AGENCY NAME(S) AND ADDRESS(ES)		10. SPONSOR/MONITOR'S ACRONYM(S)			
		11. SPONSOR/MONITOR'S REPORT NUMBER(S)			
12. DISTRIBUTION/AVAILABILITY STATEMENT Approved for public release; distribution unlimited					
13. SUPPLEMENTARY NOTES					
14. ABSTRACT					
15. SUBJECT TERMS					
16. SECURITY CLASSIFICATION OF:			17. LIMITATION OF ABSTRACT Same as Report (SAR)	18. NUMBER OF PAGES 21	19a. NAME OF RESPONSIBLE PERSON
a. REPORT unclassified	b. ABSTRACT unclassified	c. THIS PAGE unclassified			

Organo-Soluble Porphyrin Mixed Monolayer-Protected Gold Nanorods with Intercalated Fullerenes

Chenming Xue,[†] Yongqian Xu,[‡] Yi Pang,[‡] Dingshan Yu,[§] Liming Dai,[§] Min Gao,[†]

Augustine Urbas[±] and Quan Li^{,†}*

[†]Liquid Crystal Institute, Kent State University, Kent, Ohio 44242, United States, [‡]Department of Chemistry and Maurice Morton Institute of Polymer Science, The University of Akron, Akron, Ohio 44325, United States, [§]Department of Chemical Engineering, Case Western Reserve University, Cleveland, Ohio 44106, United States, [±]Materials and Manufacturing Directorate, Air Force Research laboratory WPAFB, Ohio 45433, United States

qli1@kent.edu

RECEIVED DATE (to be automatically inserted after your manuscript is accepted if required according to the journal that you are submitting your paper to)

Organo-soluble porphyrin mixed monolayer-protected gold nanorods were synthesized and characterized. The resulting gold nanorods encapsulated by both porphyrin thiol and alkyl thiol on their entire surface with strong covalent Au-S linkages were very stable in organic solvents without aggregation or decomposition, and exhibited unique optical properties different from their corresponding spherical ones. Alkyl thiol acts as a stabilizer not only to fill up the potential space on gold nanorod surface between bulky porphyrin molecules, but also to provide space for further insertion of C₆₀ molecules forming a stable C₆₀-porphyrin-gold nanorod hybrid nanostructure.

INTRODUCTION

1
2
3 Building metal nanoparticles protected by functional organic molecules is a rapidly growing
4 fascinating and challenging scientific area of contemporary interest. Gold nanorods (GNRs), providing
5 many promising applications in optics,¹ sensors,² biological imaging³ and anticancer agents⁴ due to their
6 extraordinary shape- and surface chemical environment-dependent optical properties, are among the
7 most exciting materials today. They are quite different from the widely investigated spherical gold
8 nanoparticles (GNPs),⁵ including more distinguished physical properties^{1a,6} particularly for their tunable
9 absorption in the visible and near IR region. Besides, since anisotropic metal nanoparticles can give
10 higher sensitivity than spherical ones in surface plasmon shift, GNRs are highly suitable for plasmon
11 sensing with a high-value shape factor (surface curvature).⁷ Also nanoparticle shape plays an important
12 role in surface-enhanced Raman scattering enhancement (SERS). The enhancement factors on the order
13 of 10^4 - 10^5 were observed for absorbed molecules on the GNRs, while no such enhancement was
14 observed on spherical nanoparticles under similar conditions.⁸

15
16
17
18
19
20
21
22
23
24
25
26
27
28
29
30
31 It is well established that modifying the chemical composition of GNR surfaces provides a versatile
32 means to tune their properties. For example, with dye molecules on GNRs, photothermal therapy and
33 fluorescence imaging can be accomplished simultaneously.^{4b} Although the coupling of dye molecules
34 and GNRs has been implemented via ionic interactions,⁹ the dynamically unstable bilayer
35 cetyltrimethylammonium bromide (CTAB) structure on GNRs has been a problem limiting their
36 potential applications. In these cases, thiol molecules may have an advantage because thiol monolayer-
37 protected GNRs exhibit superior stability, accessible surface functionalization and good compatibility
38 with organic media, in which they can disperse well. However, to date only a few thiol monolayer-
39 protected GNRs have been reported as the seemingly trivial work of exchanging CTAB with organic
40 thiol molecules to form thiol-monolayer-protected GNRs is challenging.¹⁰

41
42
43
44
45
46
47
48
49
50
51
52
53
54 For chemical modification of GNRs, one class of intriguing dye molecules are porphyrins, which have
55 been intensively studied for a range of applications over the decades due to their excellent thermal
56 stability, charge transport ability and high light-harvesting capability.^{11,12} It was discovered that when
57
58
59
60

1 attached to spherical GNP rather than on bulk gold surfaces, the undesirable energy transfer quenching
2 of porphyrin's singlet excited state can be suppressed.¹³ Furthermore, porphyrin and fullerene (C₆₀) are
3 an ideal donor-acceptor pair, which allows accelerated photoinduced electron transfer and slow charge
4 recombination, leading to the generation of a long lived charge-separated state with a high quantum
5 yield.¹⁴ The porphyrin-C₆₀ assemblies can be stabilized by the attractive π - π interactions.^{14b} It is the first
6 time to anchor them onto anisotropic gold nanoparticles and they are expected to present advantages for
7 solar energy conversion.
8

9
10
11
12
13
14
15
16
17 Herein we report the synthesis of GNRs that are protected by porphyrin thiol **1** and 1-decanethiol
18 molecules via strong covalent Au-S bonds on the GNR's entire surface. The resulting mixed
19 porphyrin/thiol monolayer-protected gold nanorods (**P-C₁₀-GNR**) were very stable in organic solvents
20 without aggregation or decomposition, and exhibited particular optical properties, in sharp contrast to
21 the corresponding spherical GNPs, as well as, the porphyrin thiol **1**. The alkyl thiol C₁₀H₂₁SH acts as a
22 stabilizer not only to fill up the potential space on GNR surface between bulky porphyrin molecules, but
23 also to provide space for further insertion of C₆₀ molecules. Owing to the presence of C₁₀H₂₁SH
24 molecules, the shorter alkyl chains create void space between bulky porphyrin groups for C₆₀ molecules,
25 resulting in an electron donor-acceptor structure on the GNR surface. Together with **P-C₁₀-GNR**, single
26 porphyrin monolayer-protected gold nanorods (**P-GNR**), C₁₀H₂₁SH monolayer-protected gold nanorods
27 (**C₁₀-GNR**), and porphyrin monolayer-protected spherical gold nanoparticles (**P-GNP**) were also
28 synthesized for comparison study (see supporting information). Compared with the straightforward
29 synthesis of spherical **P-GNPs** in one step,¹⁵ the preparation of thiol monolayer-protected GNRs is more
30 complicated.
31
32
33
34
35
36
37
38
39
40
41
42
43
44
45
46
47
48

49 EXPERIMENTAL SECTION

50
51
52 **Materials and Measurements.** All chemicals and solvents were purchased from commercial supplies
53 and used without further purification. HAuCl₄ is a 30 wt% in diluted HCl solution. ¹H NMR spectra
54 were recorded on a Bruker 400 MHz NMR spectrometer, with deuterated chloroform (CDCl₃) as solvent
55 at 25 °C. The chemical shifts were reported using 7.26 ppm of CHCl₃ residue as the internal standard.
56
57
58
59
60

¹³C NMR spectra were recorded on a Varian 200 MHz NMR spectrometer, with deuterated chloroform (CDCl₃) as solvent. The chemical shifts were reported using 77.16 ppm of CHCl₃ residue as the internal standard. The NMR graphs and data were collected by using Spinworks 3 software. Fourier transfer infrared spectra (FTIR) were recorded on a Nicolet Magna-IR™ spectrometer 550 spectrometer at the resolution of 4 cm⁻¹. High resolution mass spectrometry (HRMS) was performed by Mass Spectrometry & Proteomics Facility of Ohio State University. Elementary analysis was performed in Robertson Microlit Laboratories. UV-visible spectra were collected on a PerkinElmer Lambda 25 UV-Vis spectrometer at the resolution of 1 nm. Fluorescence spectra were recorded on a FluoroMax-4 spectrofluorometer of Horiba scientific. The Raman spectra are obtained with a RENISHAW inVia Raman microscope instrument using a diode laser with excitation wavelength of 785 nm. Samples for Raman spectra were casted on glass slides and left to dry before measurements. Each spectrum is obtained in 10 s collection time with five accumulations. For transmission electron microscopy (TEM) observation, solution samples were first dispersed on TEM Cu grids pre-coated with thin carbon film (Cu-400 CN) purchased from Pacific Grid Tech. After completely dried, they were studied using a FEI Tecnai TF20 FEG TEM equipped with a EDAX energy-dispersive X-ray spectrometer (EDX) for elemental analysis.

Preparation of Porphyrin Thiol 1. The route of preparing porphyrin thiol **1** was shown in Figure 1. The porphyrin thiol **1** was synthesized starting from unsymmetrical porphyrin derivative **2**, which was reacted with 11-bromo-1-undecanol to give bromo compound **3**. Then the active bromide **3** was reacted with potassium thiol acetate to give the intermediate compound **4**. Finally the intermediate **4** was deprotected in the presence of tetrabutylammonium cyanide (TBACN) to afford the product porphyrin thiol **1**. The structure of intermediate **2-4** was identified by ¹H NMR, ¹³C NMR, Ft-IR, elemental analysis and HRMS. For **1**, because it was not able to be purified through column, the reaction product of **1** was characterized by ¹H NMR and HRMS, from which the yield and rightness of the compound **1** can be verified (Figure S1). The details were listed in supporting information.

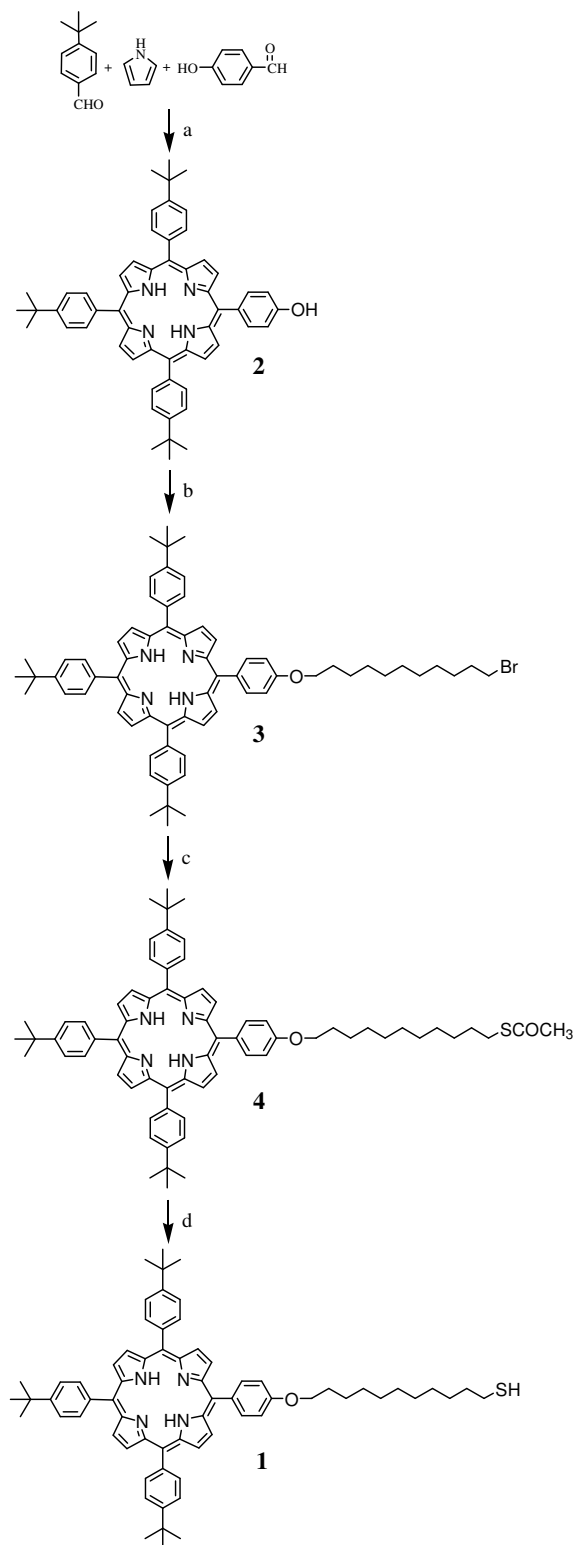


Figure 1. Synthesis of porphyrin thiol **1**. Conditions: (a) propionic acid, reflux; (b) 11-bromo-1-undecanol, DIAD, PPh₃, stir at RT; (c) CH₃COSK, acetone/CHCl₃ (1:1), RT, 24h; (d) tetrabutylammonium cyanide, CHCl₃/MeOH (2:1), 50°C, 24h.

1
2
3
4
5
6
7
8
9
10
11
12
13
14
15
16
17
18
19
20
21
22
23
24
25
26
27
28
29
30
31
32
33
34
35
36
37
38
39
40
41
42
43
44
45
46
47
48
49
50
51
52
53

Preparation of CTAB-Coated Gold Nanorods (CTAB-GNRs). The CTAB-coated GNRs were freshly prepared by the seed-mediated growth method.^{1a} For seed preparation, specifically, 0.5 mL of an aqueous 0.01 M solution of HAuCl₄ was added to CTAB solution (15 mL, 0.1 M) in a vial. A bright brown-yellow color was appeared. Then, 1.20 mL of 0.01 M ice-cold aqueous NaBH₄ solution was added all at once, followed by rapid inversion mixing for 2 minutes. The solution developed a pale brown-yellow color. Then, the vial was kept in a water bath maintained at 25 °C for future use. For nanorods growth, 9.5 mL of 0.1 M CTAB solution in water was added to a tube, 0.40 mL of 0.01 M HAuCl₄ and 0.06 mL of 0.01 M AgNO₃ aqueous solutions were added in this order and mixed by inversion. Then, 0.06 mL of 0.1 M of ascorbic acid solution was added and the resulting mixture at this stage becomes colorless. The seed solution (0.02 mL) was added to the above mixture tube, and the tube was slowly mixed for 10 seconds and left to sit still in the water bath at 25-30 °C for 3 h. The final solution turned purple within minutes after the tube was left undisturbed.

28
29
30
31
32
33
34
35
36
37
38
39
40
41
42
43
44
45
46
47
48
49
50
51
52
53

Porphyrin thiol monolayer protected gold nanorods (P-GNRs). The solution of CTAB-GNRs was centrifuged at 7500 rpm per 20 minutes several times to remove the excessive CTAB and other solution components and redispersed in 1.5 mL of water. Then, this aqueous solution of GNRs was added dropwise to a solution of the thiol **1** (50 mg) in 40 mL THF with stirring under the protection of nitrogen. The color of the reaction mixture is purple. The reaction mixture was continued to stir at room temperature for 3 days and centrifuged. To improve the GNRs with thiol molecules over the surface, the precipitates were dispersed in CHCl₃ and sonicated, 10 mg thiol **1** were added into the solutions. The solution was stirred for another 24 h and centrifuged. This procedure was repeated another three times. The as-prepared GNRs were centrifuged and washed with CHCl₃ several times until there was no UV or ¹H NMR signal in the top layer solution, which means there were no free thiols in the system. The resulting GNRs were named as **P-GNRs**.

54
55
56
57
58
59
60

Decanethiol monolayer protected gold nanorods (C₁₀-GNRs). The synthesis method was following the above, the thiol molecules C₁₀H₂₁SH (30 mg) was used for the first exchange and 10 mg was used for each of the next steps for complete surface protection.

1 **Porphyrin thiol and decanethiol monolayer protected gold nanorods (P-C₁₀-GNRs).** The
2 synthesis method was following the above, the porphyrin thiol **1** (56 mg, 0.057 mmol) was mixed with
3 CTAB-GNR first and then C₁₀H₂₁SH (10 mg, 0.057 mmol) was added slowly. 5 mg **1** and 10 mg
4 C₁₀H₂₁SH were used for each of the next steps for complete surface protection.
5
6
7
8

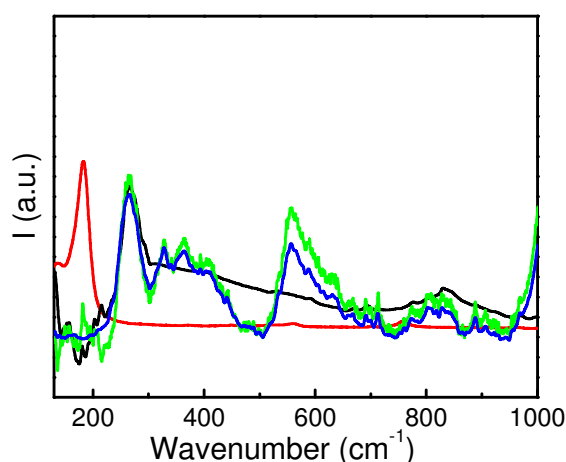
9 **Synthesis of Porphyrin-Thiol Monolayer Protected Spherical Gold Nanoparticles (P-GNPs).** The
10 route is based on the reference^{15a} with some modifications. An aqueous solution of hydrogen
11 tetrachloroaurate (3 mL, 30 mmol/L) was mixed with a solution of tetraoctylammonium bromide in
12 toluene (8 mL, 50 mmol/L). The two-phase mixture was vigorously stirred until all the tetrachloroaurate
13 was transferred into the organic layer. The water layer was removed and 50 mg **1** was then added to the
14 organic phase. A freshly prepared aqueous solution of sodium borohydride (2.5 mL, 0.4 mol/L) was
15 slowly added with vigorous stirring. After further stirring for 3 h the organic phase was separated,
16 evaporated to 1ml in a rotary evaporator and mixed with 40 ml ethanol. The mixture was kept for 4 h at
17 -18°C. The crude product was filtered off and washed with ethanol. The solid was dissolved in CHCl₃
18 and centrifuged at 14000 rpm for 12 min. After centrifuge, the top layer was removed and the solid was
19 sonicated after adding CHCl₃. This wash step was carried several times until the top layer does not have
20 UV or vis absorption signal for free porphyrin molecules. Afterwards, the **P-GNP** in CHCl₃ was
21 obtained.
22
23
24
25
26
27
28
29
30
31
32
33
34
35
36
37
38
39

40 **Preparation of C₆₀-P-C₁₀-GNR.** For inserting fullerenes (C₆₀) into the **P-C₁₀-GNR** or **P-GNR**, about
41 0.4 mg corresponding NRs was dissolved in 2 mL of 1:1 (v/v) toluene/CH₃CN. Saturated C₆₀ toluene
42 solution (3 mg/mL) was added by drops. The mixture was stirred at room temperature. The prepared
43 **C₆₀-P-C₁₀-GNR** and **C₆₀-P-GNR** solutions were centrifuged. Then the top layer was removed, 2 mL of
44 CHCl₃ was added and the mixture was sonicated. After washed with CHCl₃ several times until there was
45 no UV absorption in the top layer, which means there was no free C₆₀ in the solvent. CHCl₃ (2 mL) was
46 added and the solid was sonicated and dispersed well.
47
48
49
50
51
52
53
54
55

56 **I₂ Induced Decomposition of P-C₁₀-GNR.** In a typical procedure, ca. 2 mg **P-C₁₀-GNR** were
57 dissolved in CDCl₃ and its ¹H NMR spectrum was collected. Then, 1 mg iodine was added to this
58
59
60

1 solution and followed by stirring at room temperature for 3 h. The decomposition process could be
2 monitored by a change in solution color from purple to dark red-purple. After removal of bulky gold by
3 centrifuging, the clear top layer solution was collected and dried. After dissolved in CDCl_3 , ^1H NMR
4 spectrum was collected and it was compared with that from before decomposition. For fluorescence
5 experiment, since the excess I_2 made the solution pink-red color, aqueous $(\text{NH}_4)_2\text{SO}_3$ solution (0.5 M)
6 was added to the above organic solution and it was shaken vigorously. Afterwards, the aqueous layer
7 was removed. P-GNP and P-GNR were treated the same way for releasing porphyrin thiols.
8
9
10
11
12
13
14
15

16 RESULTS AND DISCUSSION



34 **Figure 2.** Raman spectra of the **CTAB-GNR** (red), **P-C₁₀-GNR** (blue), **P-GNR** (green), and **C₁₀-GNR**
35 (black).
36
37

38
39
40 Raman spectra (Figure 2) exhibited a characteristic Au-Br band at 180 cm^{-1} for CTAB-coated gold
41 nanorods (**CTAB-GNR**) and a characteristic Au-S band at 260 cm^{-1} accompanied with the
42 disappearance of Au-Br band for **P-C₁₀-GNR**, **P-GNR** and **C₁₀-GNR**,^{8,16} which indicated the successful
43 removal of bromide and covalent bonding of thiol molecule to gold surface. In order to further confirm
44 that the thiol molecules indeed replaced CTAB molecules on GNR surface, energy-dispersive X-ray
45 spectroscopy (EDX) was performed (Figure S2). It can be seen that the S peak appeared for **P-C₁₀-GNR**
46 with the disappearance of Br peak. Besides, ^1H NMR (Figure 3) measurements show the peaks became
47 broadened and weaker than the free porphyrin **1** molecules, similar to the results of other GNRs.^{10c} The
48 reasons for this broadening effect have been raised: (a) the tight packing of protons close to the Au core
49 causes rapid spin-spin relaxation from dipolar interactions; (b) there are different chemical shifts for
50 surface heterogeneities (different nanocrystalline faces: vertexes, edges, terraces), and the chemical
51 shifts vary with core size and defect; and (c) slow rotational diffusion of the clusters (analogous to
52
53
54
55
56
57
58
59
60

effects seen for large proteins) depending on nanoparticle size.^{10e} Although the signals of porphyrin thiols could not be observed on GNRs, they reappeared after been detached from GNRs. After degradation by adding I₂, the composition of thiol molecules on **P-C₁₀-GNR** can be calculated (Figure 3). The following is the way to calculate the ratio of porphyrin **1** to C₁₀H₂₁SH. In the green curve, the ratio of integration areas of aromatic part to alkyl part equals to 1:3. Since for porphyrin thiol **1** the porphyrin core part has 24 H (aromatic) and alkyl part has 50 H, we can calculate the integration of protons from C₁₀H₂₁SH equal to: $3 - 1/24 \times 50 = 0.92$ from the green curve (as the integration of porphyrin aromatic H = 1). Therefore, the ratio of **1** to C₁₀H₂₁SH is (1/24):(0.92/22), approximately 1 : 1. Thus, it is 1:1 ratio of thiol **1** to C₁₀H₂₁SH on **P-C₁₀-GNR**.

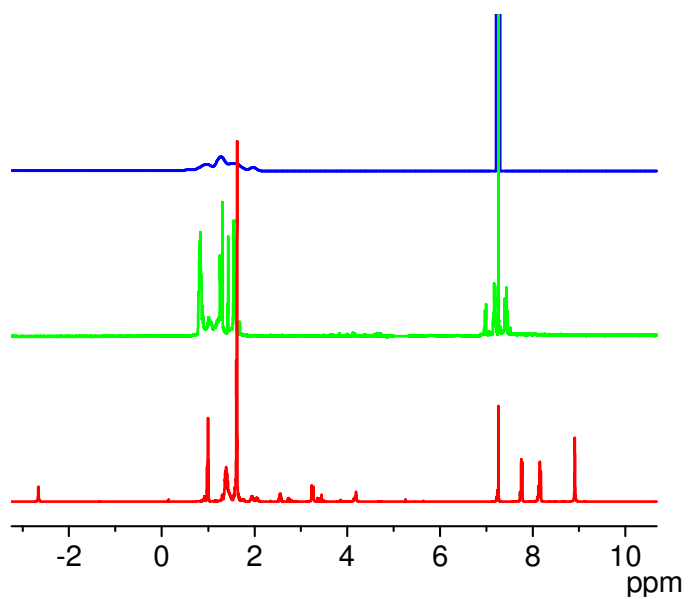
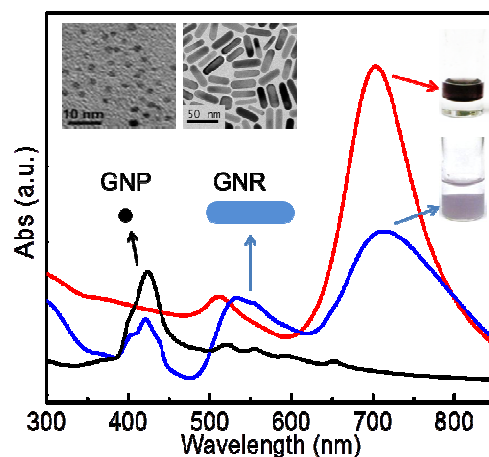


Figure 3. ¹H NMR spectra of: **P-C₁₀-GNR** (blue), mixture residue after I₂ induced decomposition (green), **1** after reducing reaction (red).



1 **Figure 4.** UV-Vis spectra of **CTAB-GNR** in H₂O (red), and **P-C₁₀-GNR** (blue) and spherical **P-GNP**
2 (black) in CHCl₃. The insets show photographs of the solutions of corresponding **CTAB-GNR** (right-
3 top) and **P-C₁₀-GNR** (right-bottom) in the two phases (top layer: water; bottom layer: CHCl₃), and TEM
4 images of **P-GNP** (left) and **P-C₁₀-GNR** (right).
5
6
7
8
9

10 UV-vis absorption spectra of **CTAB-GNR**, **P-C₁₀-GNR** and spherical **P-GNP** are shown in Figure 4.
11 Stable organo-soluble **P-C₁₀-GNR** and spherical **P-GNP** were observed by transmission electron
12 microscopy (TEM), showing they were well dispersed with no aggregation (Insets in Figure 4). **P-C₁₀-**
13 **GNR** displayed an average size of 44 nm × 13 nm and an approximate aspect ratio of 3.4 based on a
14 sample of 500 nanorods. Spherical **P-GNP** had an average diameter of 2.3 nm. The existence of typical
15 porphyrin peak at 421 nm indicated the bonding of porphyrin thiol **1** on GNR. After a successful
16 exchange with thiols, the nanoparticles were moved from aqueous media to organic solvent. In contrast
17 to UV-vis absorption spectrum of the spherical **P-GNP**, two characteristic plasmon peaks were observed
18 for both **CTAB-GNR** and **P-C₁₀-GNR**. The strong longitudinal peak in the near-infrared region (710
19 and 714 nm respectively) is corresponding to the electron oscillation along the long axis, and a weak
20 transverse peak in the visible region (513 and 533 nm respectively) is due to electron oscillation along
21 the short axis. The red-shift of the longitudinal and transverse peaks for **P-C₁₀-GNR** results from the
22 change of dielectric constant around GNR due to attachment of the porphyrin **1**. Without porphyrin **1**,
23 **C₁₀-GNR** did not show such red shift for either of these two peaks (Figure 5). Notably, the transverse
24 peak shows a large red-shift (about 20 nm), which could be ascribed to the side-by-side arrangement of
25 nanorods in solution.¹⁷ However, since there was neither accompanying blue-shift of the longitudinal
26 band, nor any prominent side-by-side assembly of GNRs observed by TEM (Inset of Figure 4 and Figure
27 S3), the peak shift can only be attributed to the influence of porphyrin **1**. Additionally, UV-vis absorption
28 spectra and TEM images of **P-GNR** (with only porphyrin **1** on GNR surface) were shown in Figure 6.
29 The appearance of characteristic porphyrin peak (421 nm) indicated the binding of **1** onto these GNRs.
30 However, its CHCl₃ solution displayed bluish color and UV-vis absorption spectra showed that the two
31
32
33
34
35
36
37
38
39
40
41
42
43
44
45
46
47
48
49
50
51
52
53
54
55
56
57
58
59
60

1
2
3
4
5
6
7
8
9
10
11
12
13
14
15
16
17
18
19
20
21
22
23
24
25
26
27
28
29
30
31
32
33
34
35
36
37
38
39
40
41
42
43
44
45
46
47
48
49
50
51
52
53
54
55
56
57
58
59
60

SPR peaks broadened. Also there were significant red-shift for transverse SPR (from 520 to 557 nm) and blue shift for longitudinal SPR (from 722 to 705 nm). This implies the side-by-side assembling of GNRs, which was observed by TEM. The attractive π - π interaction of porphyrin chromophores could be the interpretation for the assembly of **P-GNR**.

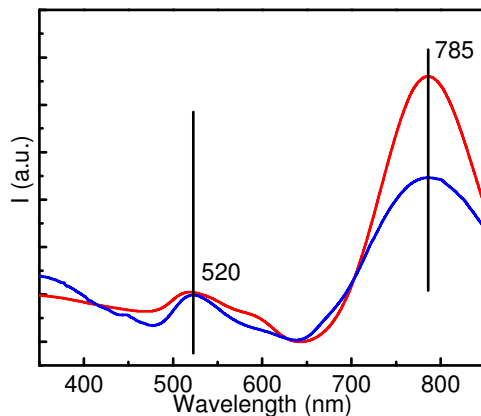


Figure 5. The UV-Vis spectra of **CTAB-GNR** in H_2O (red) and **C₁₀-GNR** in CHCl_3 (blue).

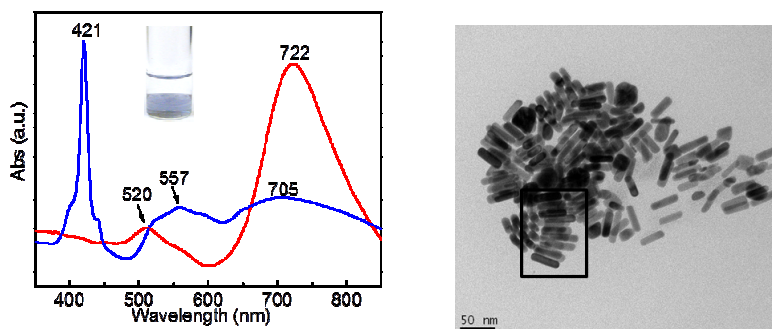


Figure 6. Left: UV-vis of **CTAB-GNR** (red) and **P-GNR** (blue) (Inset: the picture of **P-GNR** in CHCl_3 showing bluish color, top layer is water). Right: TEM image of **P-GNR**, indicating the existence of side-by-side assembly.

Fluorescence spectra (Figure 7(a), (b)) also revealed the distinctively different patterns for all these prepared nanoparticles. After detaching from gold nanoparticles, free porphyrin thiols in CHCl_3 showed characteristic emission peaks at 656 and 721 nm. When being linked onto gold nanoparticles including GNPs and GNRs, the intensity significantly quenched, almost 99%. However, for P-GNP the peak shape was almost same as free porphyrins. For P-GNR and P-C10-GNR, the peak intensity and shape were similar. Different from free porphyrins and P-GNP, the peak at 712 nm was relatively much stronger

than the 656 nm peak. This indicated that there exist the interaction between the porphyrin and gold nanoparticles, and the photoelectronic properties of porphyrin chromophores are significantly altered when closely bound to GNRs.

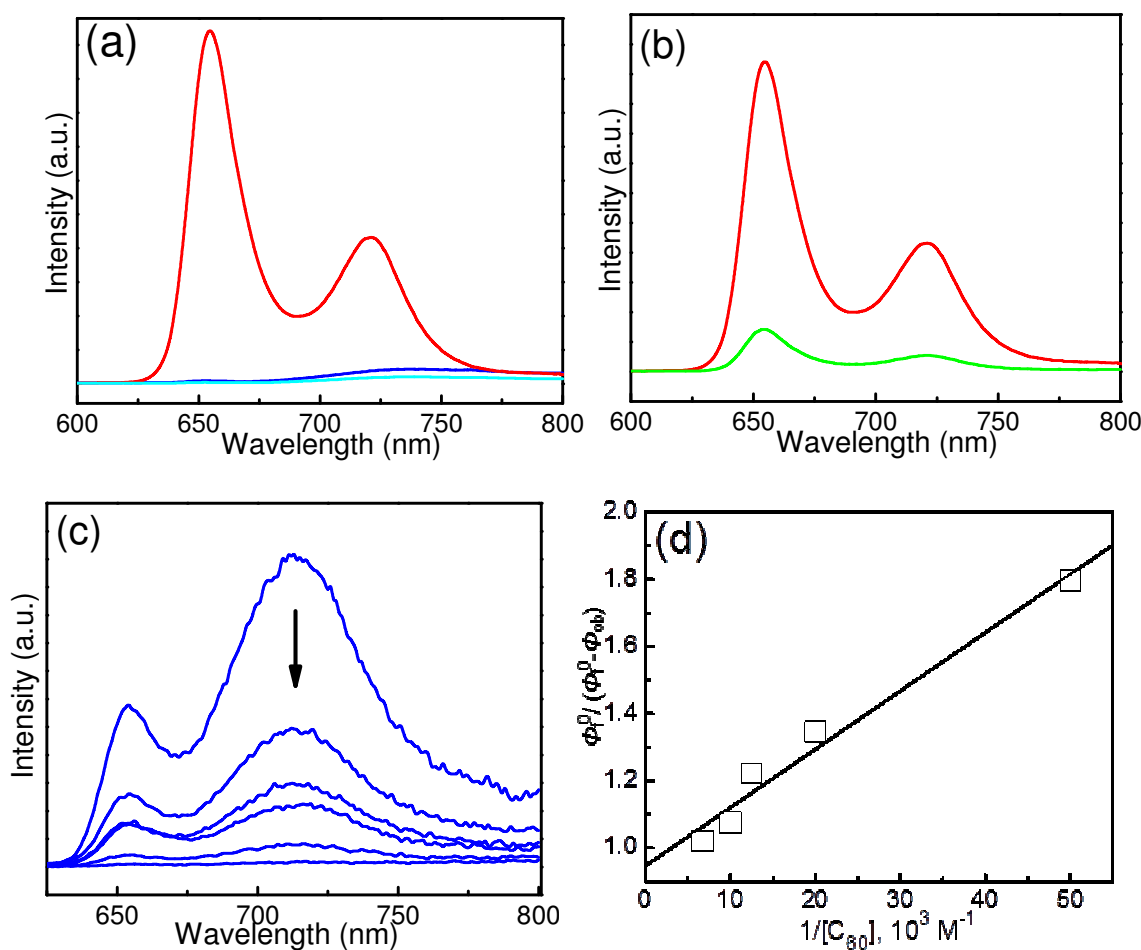
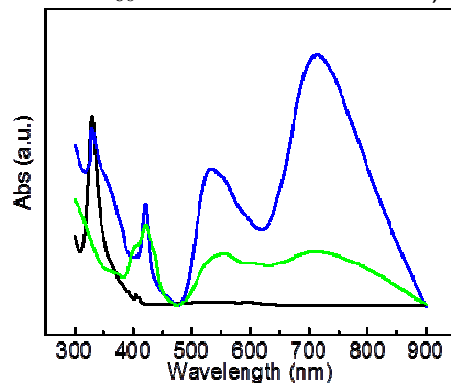


Figure 7. (a). Fluorescence spectra of free porphyrins detached from P-C₁₀-GNR (red) (diluted for ten times), P-C₁₀-GNR (blue) and P-GNR (cyan) in CHCl₃ with excitation wavelength at 420 nm. For, P-GNR the intensity of free porphyrin thiols was normalized to be the same as from P-C10-GNR. (b) Fluorescence spectra of free porphyrins detached from P-GNP (red) (diluted for ten times), P-GNP (green) in CHCl₃ with excitation wavelength at 420 nm. (c): The quench of P-C₁₀-GNR in 1:1 (v/v) toluene/CH₃CN (0.2 mg in 2 mL mixture) upon the addition of C₆₀ (C₆₀ concentrations from top to bottom: 0 mM, 0.02 mM, 0.05 mM, 0.08 mM, 0.1 mM and 0.15 mM). (d) Dependence of $\Phi_f^0 / (\Phi_f^0 - \Phi_f^{ob})$ on the reciprocal concentration of C₆₀ in acetonitrile/toluene) 1/1.



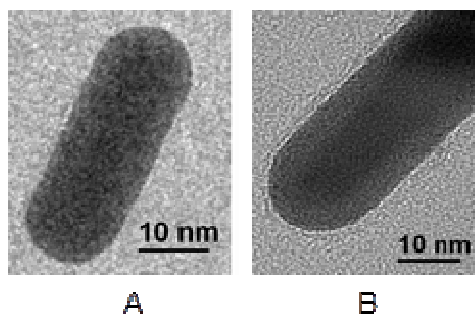


Figure 8. (Top): UV-vis spectra of **P-C₁₀-GNR** (blue) and **P-GNR** (green) after washing away free C₆₀ in solution. Solution of C₆₀ (black) has also been presented for referring. (Bottom) TEM images of **P-C₁₀-GNR** (A) and **C₆₀-P-C₁₀-GNR** conjugate. Note: The diffusion layer on the edge of **P-C₁₀-GNR** (B) indicates the existence of C₆₀ molecules.

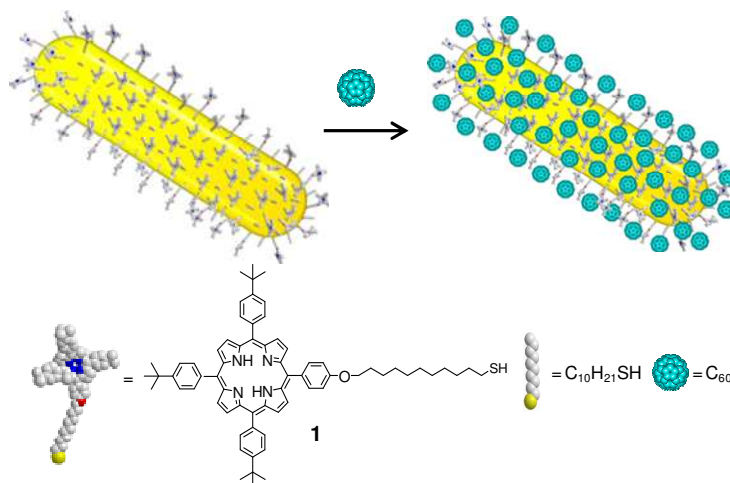
The formation of C₆₀-GNR conjugations was verified by further fluorescence quenching in toluene/CH₃CN mixture for **P-C₁₀-GNR** in Figure 7(c), even though the fluorescence of porphyrin chromophores has been significantly quenched by GNRs. (The association constant for the formation of **P-C₁₀-GNR** and C₆₀ complex has been calculated based on the fluorescence quenching in Figure 7 (c) and (d). After simplified treatment,¹⁸ the formular is:

$$\frac{1}{\Phi_f^0 - \Phi_{f(ob)}^0} = \frac{1}{\Phi_f^0 - \Phi_f'} + \frac{1}{K(\Phi_f^0 - \Phi_f')[C_{60}]}$$

Φ_f^0 is the fluorescence quantum yield of uncomplexed P-C₁₀-GNR, Φ_f' is the complexed one, $\Phi_{f(ob)}^0$ is the observed yield and K is the association constant. Φ_f' is considered as 0 when complex is completely formed. By using this equation, a linear dependence of $1/(\Phi_f^0 - \Phi_{f(ob)}^0)$ on the concentration of C₆₀ can be obtained. After linear fit, the constant K is calculated from the slope. The K value is 58600 M⁻¹.

After removing free C₆₀ in solution by repeated centrifugation and ultrasonication, the successful intercalation of C₆₀ on **P-C₁₀-GNR** was further examined by monitoring their characteristic UV-vis absorption spectra peak (see Figure 8 top), whereas spectroscopic evidence of C₆₀ could not be found in **P-GNR** when insertion of C₆₀ was performed under the same experimental conditions. TEM provides direct evidence for the C₆₀ intercalation. As shown in Figure 8 bottom, a sharp boundary can be observed between the edge of **P-C₁₀-NR** and the supporting carbon film (A), while a thin layer can be

1 identified on the nanorod surface (B) after the addition of C_{60} followed by removing free C_{60} molecules
2 in solution, supporting the conjecture of the sandwiched C_{60} molecules in the hybrid GNRs. The
3 combination of $C_{10}H_{21}SH$ molecules and **P-C₁₀-GNR** enabled the insertion of C_{60} , creating the electron
4 donor-acceptor alternative structure on the GNR surface. A schemetic illustration of this hybrid structure
5 donor-acceptor alternative structure on the GNR surface. A schemetic illustration of this hybrid structure
6 has been presented in Figur 9.
7
8
9
10



21
22
23
24
25
26
27
28
29 **Figure 9.** Schemetic representation of **P-C₁₀-GNR** intercalated with C_{60} and chemical structure of our
30 synthesized porphyrin thiol **1** and commercially available 1-decanethiol.
31
32
33

34 Structural details of thiol molecules on **P-C₁₀-GNR** and **P-GNR** were described in Figure 10, which
35 showed the feasibility of intercalating C_{60} between porphyrin molecules on **P-C₁₀-GNR** but not on **P-**
36 **GNR**. Due to the curvature of the small spherical GNPs (*ca.* 2 nm), there was a suitable void space for
37 C_{60} to insert between two porphyrin groups.¹⁸ In the case of **P-GNR**, the surface curvature is insufficient
38 to provide such a void space. On GNR surface, the average distance between two gold atoms to which
39 thiol molecules are attached is about 5 Å.¹⁹ For **P-C₁₀-GNR**, between two **1** molecules it is about 10 Å
40 with one $C_{10}H_{21}SH$ molecule standing in the middle. From center of porphyrin **1** to the surface of GNR,
41 it is about 26 Å and the longest chain length of $C_{10}H_{21}SH$ is 13.4 Å away from the GNR surface. It can
42 be calculated as 12.6 Å from the center of porphyrin ring to $C_{10}H_{21}SH$ chain, which is much larger than
43 7.1 Å, the diameter of a C_{60} molecule.¹⁸ The closest distance between a carbon of C_{60} and the center of
44 the porphyrin ring has been reported as 2.856 Å.²⁰ The smallest center-to-center distance of two
45
46
47
48
49
50
51
52
53
54
55
56
57
58
59
60

porphyrin chromophores which can sandwich a C_{60} molecule is about 12.8 Å by adding the diameter of C_{60} to twice the closest distance between C_{60} and a porphyrin ring. With the flexible n-alkyl part of **1** which has 11 CH_2 units, the two **1** molecules on **P-C₁₀-GNR** can tilt slightly to accommodate a C_{60} molecule, as shown in the top left picture. On the other hand, for **P-GNR**, since there is no short chain on the surface to provide the void space, C_{60} molecules could not be sandwiched by porphyrin molecules. The section view of GNR has also been presented to illustrate the feasible intercalation of C_{60} on **P-C₁₀-GNR** and infeasible intercalation on **P-GNR**. The lengths of porphyrin molecule **1** and $C_{10}H_{21}SH$ were calculated in Chem 3D of ChemDraw.

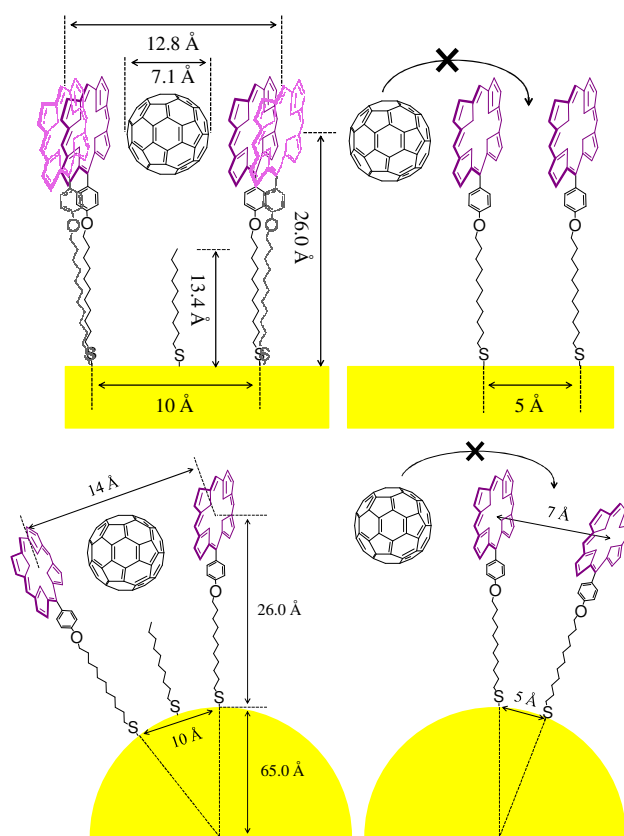


Figure 10. Schematic interpretation of feasible intercalation of C_{60} into **P-C₁₀-GNR** instead of **P-GNR**.

The top pictures are from the side view of GNR, and the bottom pictures are from the section view. The *t*-butylphenyl groups at porphyrin core are omitted for clarity.

CONCLUSION

In conclusion, porphyrin mixed monolayer-protected GNRs were for the first time synthesized and characterized. The resulting porphyrin GNRs showed unique optical properties in sharp contrast to their

1 corresponding spherical GNPs. With the short alkyl thiol molecules, **P-C₁₀-GNR** enabled the insertion
2 of C₆₀, creating the electron donor-acceptor alternative structure on the GNR surface. Through this
3 hybrid nanomaterial, it opens a new avenue for research in investigating the effects of functional organic
4 molecules on the plasmonic properties of anisotropic gold nanoparticles. This hybrid structure holds
5 promise for energy conversion in hybrid photovoltaic devices by providing increasing donor-acceptor
6 interface for the porphyrin-C₆₀ system with the huge contact area. In addition, for the future study, when
7 shorten the alkyl of porphyrin thiols and *n*-alkyl chains which pull the porphyrin groups and C₆₀
8 molecules closer to GNR surface (<1 nm), the nanorod structure could be used as a direct path for
9 charge transport, a key requirement for efficient photovoltaic devices. This combination of organic
10 electron donor-acceptor system and inorganic NRs could be used to enhance the capability of
11 photovoltaic devices and improve their performances.
12
13
14
15
16
17
18
19
20
21
22
23
24

25 26 27 ACKNOWLEDGMENT

28
29
30
31 This work was supported by the Air Force Office of Scientific Research (AFOSR FA9550-09-1-
32 0254). Discussions with X. Ma and Y. Li were acknowledged. The TEM data were obtained at the
33 (cryo) TEM facility at the Liquid Crystal Institute, Kent State University, supported by the Ohio
34 Research Scholars Program Research Cluster on Surfaces in Advanced Materials.
35
36
37
38
39
40

41 **Supporting Information Available:** Details of thiol synthesis, the interpretation of successful
42 synthesis of **1**, Raman spectra, EDX spectra and TEM images of **P-C₁₀-GNR** with larger size scale bars.
43 This material is available free of charge via the Internet at <http://pubs.acs.org>.
44
45
46
47
48

49 REFERENCES

50
51
52 (1) (a) Murphy, C. J.; San, T. K.; Gole, A. M.; Orendorff, C. J.; Gao, J. X.; Gou, L.; Hunyadi, S. E.;
53 Li, T. Anisotropic Metal Nanoparticles: Synthesis, Assembly, and Optical Applications. *J. Phys. Chem.*
54 *B* **2005**, *109*, 13857-13870. (b) Burda, C.; Chen, X. B.; Narayanan, R.; El-Sayed, M. A. Chemistry and
55 Properties of Nanocrystals of Different Shapes. *Chem. Rev.* **2005**, *105*, 1025-1102. (c) Zhou, J.; Dong,
56
57
58
59
60

1 J.; Wang, B.; Koschny, T.; Kafesaki, M.; Soukoulis, C. M. Negative Refractive Index due to Chirality.

2
3 *Phys. Rev. B* **2009**, *79*, 121104.

4
5 (2) (a) Li, C. Z.; Male, K. B.; Hrapovic, S.; Luong, J. H. T. Fluorescence Properties of Gold
6 Nanorods and Their Application for DNA Biosensing. *Chem. Commun.* **2005**, 3924-3926. (b) Yu, C. X.;
7 Irudayaraj, J. Multiplex Biosensor Using Gold Nanorods. *Anal. Chem.* **2007**, *79*, 572-579. (c) Sudeep, P.
8 K.; Joseph, S. T. S.; Thomas, K. G. Selective Detection of Cysteine and Glutathione Using Gold
9 Nanorods. *J. Am. Chem. Soc.* **2005**, *127*, 6516-6517.

10
11 (3) (a) Huang, X. H.; El-Sayed, I. H.; Qian, W.; El-Sayed, M. A. Cancer Cell Imaging and
12 Photothermal Therapy in The Near-Infrared Region by Using Gold Nanorods. *J. Am. Chem. Soc.* **2006**,
13 *128*, 2115-2120. (b) Pissuwan, D.; Valenzuela, S. M.; Miller, C. M.; Cortie, M. B. A Golden Bullet?
14 Selective Targeting of Toxoplasma Gondii Tachyzoites Using Anti Body-Functionalized Gold
15 Nanorods. *Nano Lett.* **2007**, *7*, 3808-3812. (c) Ding, H.; Yong, K. T.; Roy, I.; Pudavar, H. E.; Law, W.
16 C.; Bergey, E. J.; Prasad, P. N. Gold Nanorods Coated with Multilayer Polyelectrolyte as Contrast
17 Agents for Multimodal Imaging. *J. Phys. Chem. C* **2007**, *111*, 12552-12557.

18
19 (4) (a) Chen, C. C.; Lin, Y. P.; Wang, C. W.; Tzeng, H. C.; Wu, C. H.; Chen, Y. C.; Chen, C. P.;
20 Chen, L. C.; Wu, Y. C. DNA-Gold Nanorod Conjugates for Remote Control of Localized Gene
21 Expression by Near Infrared Irradiation. *J. Am. Chem. Soc.* **2006**, *128*, 3709-3715. (b) Tong, L.; Zhao,
22 Y.; Huff, T. B.; Hansen, M. N.; Wei, A.; Cheng, J. X. Gold Nanorods Mediate Tumor Cell Death by
23 Compromising Membrane Integrity. *Adv. Mater.* **2007**, *19*, 3136-3141. (c) Norman, R. S.; Stone, J. W.;
24 Gole, A.; Murphy, C. J.; Sabo-Attwood, T. L. Targeted Photothermal Lysis of The Pathogenic Bacteria,
25 *Pseudomonas Aeruginosa*, with Gold Nanorods. *Nano Lett.* **2008**, *8*, 302-306.

26
27 (5) Daniel, M. C.; Astruc, D. Gold Nanoparticles: Assembly, Supramolecular Chemistry, Quantum-
28 Size-Related Properties, and Applications toward Biology, Catalysis, and Nanotechnology. *Chem. Rev.*
29 **2004**, *104*, 293-346.

1
2
3
4
5
6
7
8
9
10
11
12
13
14
15
16
17
18
19
20
21
22
23
24
25
26
27
28
29
30
31
32
33
34
35
36
37
38
39
40
41
42
43
44
45
46
47
48
49
50
51
52
53
54
55
56
57
58
59
60

(6) Link, S.; El-Sayed, M. A. Spectral Properties and Relaxation Dynamics of Surface Plasmon Electronic Oscillations in Gold and Silver Nanodots and Nanorods. *J. Phys. Chem. B* **1999**, *103*, 8410-8426.

(7) Yu, C.; Irudayaraj, J. Quantitative Evaluation of Sensitivity and Selectivity of Multiplex NanoSPR Biosensor Assays. *Biophys. J.* **2007**, *93*, 3684-3692.

(8) Nikoobakht, B.; Wang, J. P.; El-Sayed, M. A. Surface-Enhanced Raman Scattering of Molecules Adsorbed on Gold Nanorods: Off-Surface Plasmon Resonance Condition. *Chem. Phys. Lett.* **2002**, *366*, 17-23.

(9) Ni, W. H.; Yang, Z.; Chen, H. J.; Li, L.; Wang, J. F. Coupling Between Molecular and Plasmonic Resonances in Freestanding Dye-Gold Nanorod Hybrid Nanostructures. *J. Am. Chem. Soc.* **2008**, *130*, 6692-6693.

(10) (a) Khanal, B. P.; Zubarev, E. R. Rings of Nanorods. *Angew. Chem. Int. Ed.* **2007**, *46*, 2195-2198. (b) Dai, Q.; Coutts, J.; Zou, J. H.; Huo, Q. Surface Modification of Gold Nanorods through A Place Exchange Reaction inside An Ionic Exchange Resin. *Chem. Commun.* **2008**, 2858-2860. (c) Li, Y. N.; Yu, D. S.; Dai, L. M.; Urbas, A.; Li, Q. Organo-Soluble Chiral Thiol-Monolayer-Protected Gold Nanorods. *Langmuir* **2011**, *27*, 98-103. (d) El Khoury, J. M.; Zhou, X.; Qu, L. T.; Dai, L. M.; Urbas, A.; Li, Q. Organo-Soluble Photoresponsive Azo Thiol Monolayer-Protected Gold Nanorods. *Chem. Commun.* **2009**, 2109-2111. (e) Donkers, R. L.; Lee, D.; Murray, R. W. Synthesis and Isolation of The Molecule-Like Cluster Au₃₈(PhCH₂CH₂S)₂₄. *Langmuir* **2004**, *20*, 1945-1952.

(11) Kadish, K. M.; Smith, K. M.; Guillard, R. *Eds. The Porphyrin Handbook*, Academic Press: San Diego, **2000**.

(12) Sun, Q.; Dai, L.; Zhou, X.; Li, L.; Li, Q. Bilayer- and Bulk-Heterojunction Solar Cells Using Liquid Crystalline Porphyrins as Donors by Solution Processing. *Appl. Phys. Lett.* **2007**, *91*, 253505.

1 (13) (a) Imahori, H.; Arimura, M.; Hanada, T.; Nishimura, Y.; Yamazaki, I.; Sakata, Y.; Fukuzumi, S.
2 Photoactive Three-Dimensional Monolayers: Porphyrin-Alkanethiolate-Stabilized Gold Clusters. *J. Am.*
3 *Chem. Soc.* **2001**, *123*, 335-336. (b) Imahori, H.; Kashiwagi, Y.; Endo, Y.; Hanada, T.; Nishimura, Y.;
4 Yamazaki, I.; Araki, Y.; Ito, O.; Fukuzumi, S. Structure and Photophysical Properties of Porphyrin-
5 Modified Metal Nanoclusters with Different Chain Lengths. *Langmuir* **2004**, *20*, 73-81.
6
7
8
9
10
11

12 (14) (a) Zhou, X.; Kang, S. W.; Kumar, S.; Kulkarni, R. R.; Cheng, S. Z. D.; Li, Q. Self-Assembly of
13 Porphyrin and Fullerene Supramolecular Complex into Highly Ordered Nanostructure by Simple
14 Thermal Annealing. *Chem. Mater.* **2008**, *20*, 3551-3553. (b) Sun, D.; Tham, F. S.; Reed, C. A.; Chaker,
15 L.; Boyd, P. D. W. Supramolecular Fullerene-Porphyrin Chemistry. Fullerene Complexation by
16 Metalated "Jaws Porphyrin" Hosts. *J. Am. Chem. Soc.*, **2002**, *124*, 6604-6612 and references there in.
17
18
19
20
21
22
23
24

25 (15) (a) Brust, M.; Walker, M.; Bethell, D.; Schiffrin, D. J.; Whyman, R. Synthesis of Thiol-
26 Derivatized Gold Nanoparticles in A 2-Phase Liquid-Liquid System. *J. Chem. Soc. Chem. Commun.*
27 **1994**, 801-802. (b) Zhou, X.; El Khoury, J. M.; Qu, L.; Dai, L.; Li, Q. A Facile Synthesis of Aliphatic
28 Thiol Surfactant with Tunable Length as A Stabilizer of Gold Nanoparticles in Organic Solvents. *J.*
29 *Colloid Interf. Sci.* **2007**, *308*, 381-384.
30
31
32
33
34
35
36
37

38 (16) Huang, X. H.; Neretina, S.; El-Sayed, M. A. Gold Nanorods: From Synthesis and Properties to
39 Biological and Biomedical Applications. *Adv. Mater.* **2009**, *21*, 4880-4910.
40
41
42

43 (17) Park, H. S.; Agarwal, A.; Kotov, N. A.; Lavrentovich, O. D. Controllable Side-by-Side and End-
44 to-End Assembly of Au Nanorods by Lyotropic Chromonic Materials. *Langmuir* **2008**, *24*, 13833-
45 13837.
46
47
48
49

50 (18) Hasobe, T.; Imahori, H.; Kamat, P. V.; Ahn, T. K.; Kim, S. K.; Kim, D.; Fujimoto, A.;
51 Hirakawa, T.; Fukuzumi, S. Photovoltaic Cells Using Composite Nanoclusters of Porphyrins and
52 Fullerenes with Gold Nanoparticles. *J. Am. Chem. Soc.* **2005**, *127*, 1216-1228.
53
54
55
56
57
58
59
60

1 (19) (a) Poirier, G. E. Characterization of Organosulfur Molecular Monolayers on Au(111) Using
2 Scanning Tunneling Microscopy. *Chem. Rev.* **1997**, *97*, 1117-1127. (b) Menendez, G.; Cortes, E.;
3 Grumelli, D.; De Leo, L. P. M.; Williams, F. J.; Tognalli, N. G.; Fainstein, A.; Vela, M. E.; Jares-
4 Erijman, E. A.; Salvarezza, R. C. Self-Assembly of Thiolated Cyanine Aggregates on Au(111) and Au
5 Nanoparticle Surfaces. *Nanoscale* **2012**, *4*, 531-540.
6
7
8
9
10

11
12 (20) Sun, D. Y.; Tham, F. S.; Reed, C. A.; Chaker, L.; Burgess, M.; Boyd, P. D. W. Porphyrin-
13 Fullerene Host-Guest Chemistry. *J. Am. Chem. Soc.* **2000**, *122*, 10704-10705.
14
15
16
17
18
19
20
21
22
23
24

25 TOC:

